

## The 64th special issue "Frontiers of Carbon Materials"

### Effect of Electrolyte Additives on Kinetic Parameters of Lithium-ion Transfer Reactions at Electrolyte/Graphite Interface

Akane INOO,<sup>a</sup> Tomokazu FUKUTSUKA,<sup>b</sup> Yuto MIYAHARA,<sup>a</sup> Yasuyuki KONDO,<sup>a</sup>  
Yuko YOKOYAMA,<sup>a</sup> Kohei MIYAZAKI,<sup>a,\*</sup> and Takeshi ABE<sup>a</sup>

<sup>a</sup> Graduate School of Engineering, Kyoto University, Nishikyo-ku, Kyoto 615-8510, Japan

<sup>b</sup> Graduate School of Engineering, Nagoya University, Chikusa-ku, Nagoya 464-8603, Japan

\* Corresponding author: [myzkohei@elech.kuic.kyoto-u.ac.jp](mailto:myzkohei@elech.kuic.kyoto-u.ac.jp)

#### ABSTRACT

The performance of the graphite anode of lithium-ion batteries is greatly affected by the solid electrolyte interphase (SEI) generated at the first charge. However, there are few studies on the kinetics of the lithium-ion intercalation/de-intercalation reaction in graphite to investigate the effect of SEI. In this study, the correlation between the interfacial lithium-ion transfer resistance ( $R_{ct}$ ) and the double layer capacitance ( $C_{dl}$ ) of graphite composite electrodes coated with various SEIs was investigated. It was found that the value of  $1/R_{ct}C_{dl}$  was different for each SEI, that is, the frequency (or rate) of intercalation and de-intercalation of lithium ions into graphite was different for each SEI. The activation energy of  $R_{ct}$  was almost the same for all the electrolyte solutions. These results indicate that the pre-exponential factor of the Arrhenius equation governing the rate of interfacial ion transfer in a practical graphite anode is dependent on the nature of SEI.

© The Author(s) 2020. Published by ECSJ. This is an open access article distributed under the terms of the Creative Commons Attribution 4.0 License (CC BY, <http://creativecommons.org/licenses/by/4.0/>), which permits unrestricted reuse of the work in any medium provided the original work is properly cited. [DOI: 10.5796/electrochemistry.20-64048]. Uploading "PDF file created by publishers" to institutional repositories or public websites is not permitted by the copyright license agreement.



Keywords : Lithium-ion Transfer, Solid Electrolyte Interphase, Graphite Anode, Activation Energy

#### 1. Introduction

In recent years, lithium-ion batteries have been used as a power source for electric vehicles (EVs). In order for electric vehicles to become more widely used, it is necessary to improve the performance of lithium-ion batteries (LIBs) installed in electric vehicles. One of the key characteristics of lithium-ion batteries for practical use in electric vehicles is rate performance. In order to improve the rate performance, the kinetics of lithium-ion transfer needs to be elucidated in detail. One of the slowest steps in the process of LIBs is the transfer of lithium ions at the interface between the electrode and the electrolyte.<sup>1</sup> In particular, in graphite anode, a solid electrolyte interphase (SEI) is formed during the first charge,<sup>2,3</sup> but the properties of SEI vary depending on the solvent, salt, and additives in the electrolyte solution.<sup>4–13</sup> Since SEI covers the active site of the lithium-ion intercalation reaction on the graphite surface, the kinetics of interfacial lithium-ion transfer may be different due to the different properties of SEI. In order to improve the kinetic performance of graphite, it is important to clarify the effect of SEI on the interfacial lithium-ion transfer process.

To evaluate the above points, highly oriented pyrolytic graphite (HOPG) has been used as a model electrode to correlate the standard rate constants ( $k^0$ ) of  $[\text{Ru}(\text{NH}_3)_6]^{3+/2+}$  redox reactions, double layer capacitance ( $C_{dl}$ ) and lithium ion transfer resistance ( $R_{ct}$ ) after SEI formation with and without the addition of vinylene carbonate (VC) or fluoroethylene carbonate (FEC) in ethylene carbonate (EC).<sup>14</sup> For these electrolyte solutions,  $k^0$  and  $C_{dl}$  were found to be linearly correlated with  $1/R_{ct}$  and the slope of the line varied with the SEI-forming solvent. SEIs obtained from these electrolyte solutions and additives showed different pre-exponential factors of the Arrhenius equation of interfacial lithium-ion transfer. These results suggest that the kinetics of interfacial lithium-ion transfer is influenced by the

solvents and additives that form SEI, but it is not easy to apply the kinetics to practical LIBs. This is because graphite composite electrodes used in practical LIBs have a higher number of graphite edge sites compared to HOPG, and the results observed in HOPG are not always observable in graphite composite electrodes. Therefore, it is important to adapt the quantitative experimental methods used in the previous HOPG study to the graphite composite electrodes. However, due to the complexity of the composite electrode structure, the diffusion process of redox species within the electrode may also be complicated, which may adversely affect the analysis of  $k^0$ . In this study, the correlation between  $R_{ct}$  and  $C_{dl}$  of the graphite composite electrodes coated with various types of SEI was evaluated and the effect of SEI on the interfacial lithium-ion transfer rate was investigated.

#### 2. Experimental

Natural graphite (SNO-15, SEC carbon) was used for making a composite working electrode with a polyvinylidene difluoride binder (SNO-15:polyvinylidene difluoride = 9:1 by weight). A propylene carbonate (PC) solution of 1 mol dm<sup>-3</sup> (C<sub>2</sub>H<sub>5</sub>)<sub>4</sub>NBF<sub>4</sub> (TEABF<sub>4</sub>) was used as an electrolyte solution to measure double-layer capacitances ( $C_{dl}$ ). The organic electrolyte, TEABF<sub>4</sub>/PC, is a commonly used solution for electric double-layer capacitors.<sup>15</sup> A Li metal electrode immersed in 0.5 mol dm<sup>-3</sup> LiBF<sub>4</sub>/PC solution was used as a reference electrode, and the two solutions (TEABF<sub>4</sub>/PC and LiBF<sub>4</sub>/PC) were separated by a glass frit. Double-layer capacitance was evaluated by cyclic voltammetry in a potential range of 2.9–3.0 V (vs. Li<sup>+</sup>/Li).

Lithium-ion transfer resistance ( $R_{ct}$ ) was measured using the same cells after measuring  $C_{dl}$ . The cells were cleaned with a solution of EC and diethyl carbonate (DEC) (1:1 by volume) and

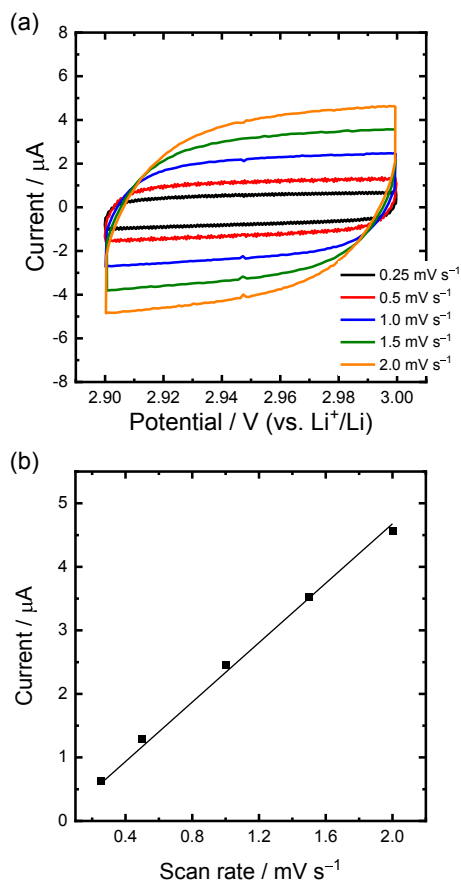


**Figure 1.** (a) Cyclic voltammograms of the graphite composite electrodes in  $1 \text{ mol dm}^{-3}$  TEABF<sub>4</sub>/PC. (b) Dependence of voltammetric currents at 2.99 V of the positive sweeps on the scan rate.

$1 \text{ mol dm}^{-3}$  LiClO<sub>4</sub>/EC+DEC (1:1 by volume) without disassembling. AC impedance measurement was conducted in solutions of  $1 \text{ mol dm}^{-3}$  LiClO<sub>4</sub>/EC+DEC with or without 3 wt% additives (VC and FEC). Prior to AC impedance spectroscopy, SEI formation was performed by cyclic voltammetry with a scan rate of  $0.1 \text{ mV s}^{-1}$  in a potential range of 0–3.0 V (vs. Li<sup>+</sup>/Li) for 2 cycles. After that, the electrode potential was lowered to 0.2 V with a rate of  $0.1 \text{ mV s}^{-1}$ , and was held at 0.2 V (vs. Li<sup>+</sup>/Li) for 24 h. AC impedance spectroscopy was conducted in a frequency range of 100 kHz to 10 mHz with an AC voltage amplitude of 5 mV at the open-circuit voltage (OCV) and 0.2 V (vs. Li<sup>+</sup>/Li).

### 3. Result and Discussion

#### 3.1 Double-layer capacitance

Figure 1(a) shows typical cyclic voltammograms of the composite graphite electrode in  $1 \text{ mol dm}^{-3}$  TEABF<sub>4</sub>/PC at different scan rates. The adsorption and desorption of TEA<sup>+</sup> on graphite were seen in the voltammograms, and the currents increased with an increase in the scan rate. Oxidation currents at 2.99 V show a linear behavior in the scan rate, as shown in Fig. 1(b), and  $C_{dl}$  can be estimated from the slope of the lines. In this case, the double-layer capacity is estimated to be  $2.40 \text{ mF}$ , which is consistent with a graphite surface area of roughly  $10 \text{ m}^2 \text{ g}^{-1}$  and an area specific capacity of a few  $\mu\text{F cm}^{-2}$ .<sup>16,17</sup>

#### 3.2 SEI formation and charge-transfer resistance

SEI formation on the graphite surface was performed by cyclic voltammetry after measuring  $C_{dl}$ . Figure 2 shows cyclic voltam-

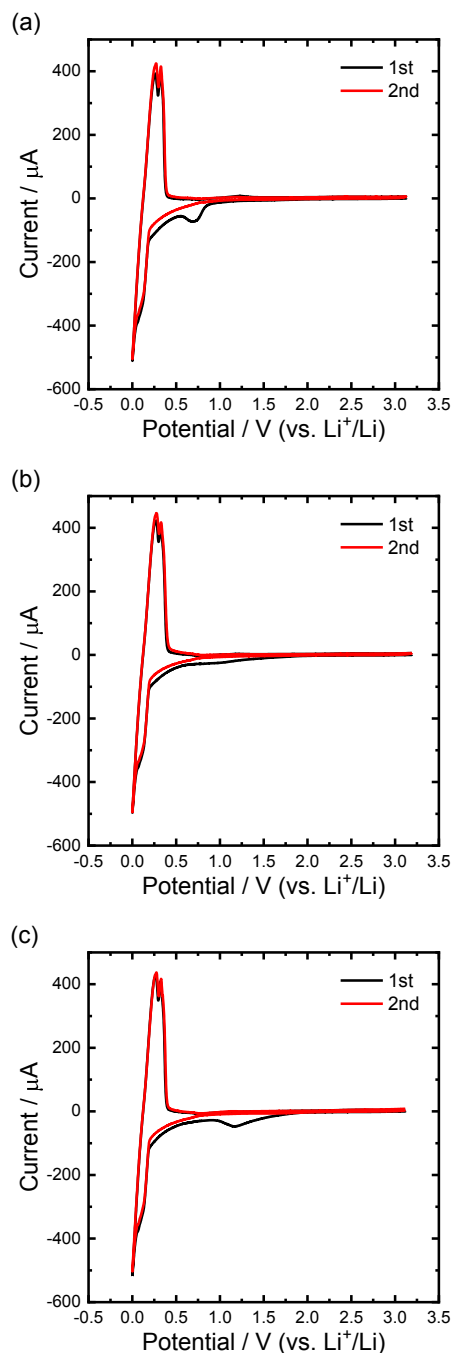


**Figure 2.** Cyclic voltammograms of the graphite composite electrodes in  $1 \text{ mol dm}^{-3}$  LiClO<sub>4</sub>/EC+DEC (1:1 by volume) containing no additive (a), VC (b), and FEC (c). Scan rate was  $0.1 \text{ mV s}^{-1}$ .

grams of the graphite composite electrodes in  $1 \text{ mol dm}^{-3}$  LiClO<sub>4</sub>/EC+DEC without (a) and with additives (b and c). In the additive-free electrolyte, the reduction peak, which corresponds to the decomposition of EC, has a maximum at around 0.7 V, shown in Fig. 2(a). On the other hand, the reduction currents in the electrolytes with VC and FEC were observed at around 1.0 and 1.2 V, respectively, in Figs. 2(b) and (c). According to the lowest unoccupied molecular orbital (LUMO), it is known that VC and FEC have relatively low LUMO level and are therefore reduced before EC.<sup>18</sup> Figure 2 shows that the reduction currents in the electrolytes containing VC and FEC were observed at a higher potential than that in the additive-free electrolyte, indicating that the

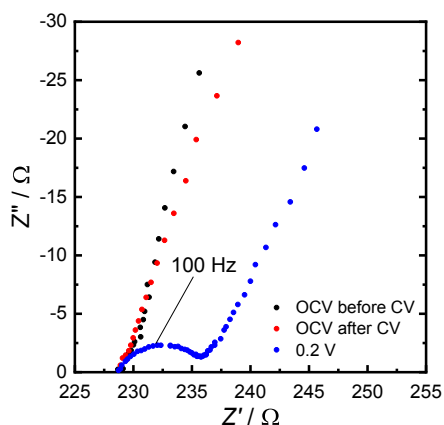


**Figure 3.** Nyquist plots of the graphite composite electrodes in  $1 \text{ mol dm}^{-3}$   $\text{LiClO}_4/\text{EC}+\text{DEC}$  (1:1 by volume) containing no additive at OCV and 0.2 V.

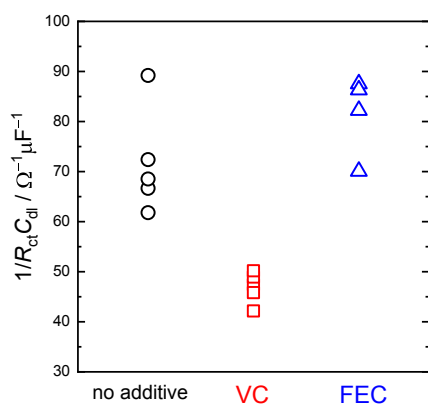


**Figure 4.** Comparing the values of  $1/R_{\text{ct}}C_{\text{dl}}$  for each SEI.

VC and FEC-derived SEI was formed on graphite. In the second cycle, almost the same current values were observed in the three electrolytes, and we confirmed that SEI formation was accomplished in the first cycle. And we prepared three kinds of graphite electrodes with different SEIs derived EC, VC, and FEC.

Figure 3 shows Nyquist plots of the graphite composite electrodes in  $1 \text{ mol dm}^{-3}$   $\text{LiClO}_4/\text{EC}+\text{DEC}$  at the potential kept of OCV and 0.2 V. In the Nyquist plots at OCV before and after CVs, the impedance changed linearly with respect to the imaginary number axis: no electrochemical reaction occurred on the graphite electrode (blocking behavior). On the other hand, a semi-circle with a characteristic frequency of 100 Hz was observed at 0.2 V, which was ascribed to the charge-transfer reaction on graphite, and Warburg impedance of  $\text{Li}^+$  diffusion was observed in a low frequency region. Similar tendencies were also observed in  $1 \text{ mol dm}^{-3}$   $\text{LiClO}_4/\text{EC}+\text{DEC}$  containing VC and FEC. Using the semi-circles observed at 0.2 V in three electrolytes,  $R_{\text{ct}}$  was evaluated by fitting the semi-circle with a RC parallel circuit.

### 3.3 Influence of SEI on lithium-ion transfer

Combining the double-layer capacitance  $C_{\text{dl}}$  and the charge-transfer resistance  $R_{\text{ct}}$ , the values of  $1/R_{\text{ct}}C_{\text{dl}}$  were plotted by the electrolytes in Fig. 4. By dividing  $1/R_{\text{ct}}$  by the measured value of  $C_{\text{dl}}$ , the surface area of graphite in contact with the electrolyte is normalized, and  $1/R_{\text{ct}}C_{\text{dl}}$  represents the frequency (or rate) of lithium-ion intercalation/de-intercalation per unit time. Therefore, we can compare the frequency of lithium-ion intercalation/

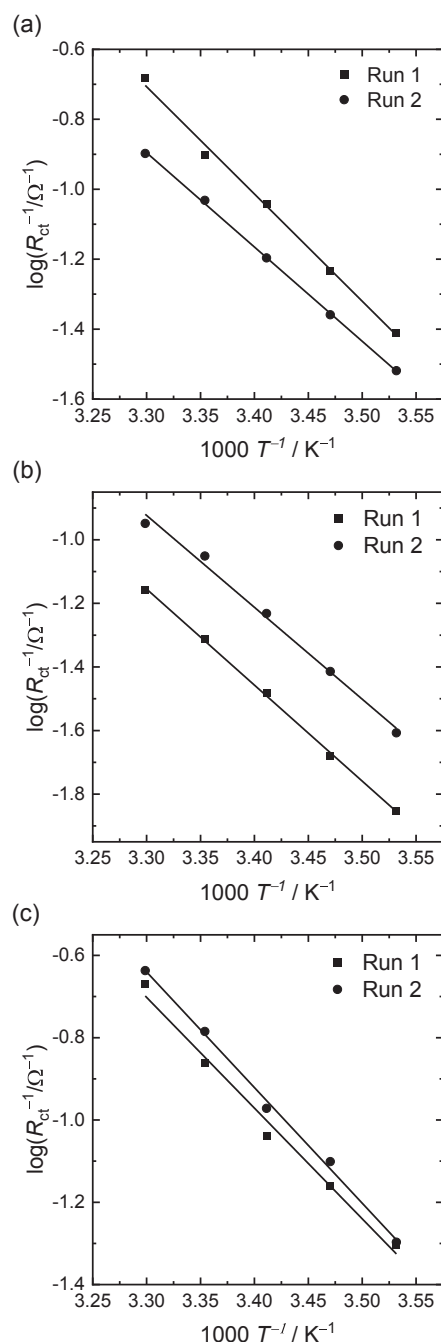


**Figure 5.** Temperature dependences of  $1/R_{\text{ct}}$  at 0.2 V (vs.  $\text{Li}^+/\text{Li}$ ) in  $1 \text{ mol dm}^{-3}$   $\text{LiClO}_4/\text{EC}+\text{DEC}$  (1:1 by volume) containing no additive (a), VC (b), and FEC (c).

deintercalation covered with each SEIs. Figure 4 shows that the value of  $1/R_{\text{ct}}C_{\text{dl}}$  increased in the order of VC, EC, and FEC. This order of  $1/R_{\text{ct}}C_{\text{dl}}$  is in good agreement with the results of previous experiments with HOPG.<sup>14</sup>

Assuming that the frequency of lithium-ion intercalation/de-intercalation follows the Arrhenius equation, the change in the frequency due to the difference in SEI could be due to the change in the activation energy or to the change in the pre-exponential factor. A higher activation energy or a decrease in the pre-exponential factor results in a decrease in the frequency of the reaction. The activation energy ( $E_a$ ) of each electrolyte was measured as the pre-exponential factor is difficult to be directly estimated. The temperature dependence of the  $R_{\text{ct}}$  obtained for each electrolyte from 10 to  $30^\circ\text{C}$  is shown in Fig. 5. With an electrode potential of 0.2 V and

SEI derived from EC, VC, and FEC, the values of  $E_a$  were 52–59, 55–58, and 52–54 kJ mol<sup>-1</sup>, respectively. In our previous reports, the activation energy of lithium-ion transfer resistance at the graphite/electrolyte interface in EC-based electrolytes was 50–60 kJ mol<sup>-1</sup>.<sup>19–21</sup> Therefore, the values of activation energy obtained in the present study were reasonable and almost the same. These results indicate that  $E_a$  does not depend on the nature of SEI, and the difference in the reaction rate of intercalation/de-intercalation may be due to the change in the pre-exponential factor. Considering the nature of the additives to form SEI here, VC is known to form a more compact film than EC and to contain more inorganic components with poor lithium-ion conductivity.<sup>22–24</sup> On the other hand, FEC-derived SEI is also dense, but it contains much LiF, which is thought to lower the interfacial resistance of graphite anode.<sup>25</sup> However, it is currently not possible to explain directly the effect of differences in the microscopic structure and chemical composition of SEI on the pre-exponential factor of the reaction frequency of lithium-ion intercalation/de-intercalation in graphite. Using the method established through this study to quantitatively compare the reaction frequencies of different SEIs, we plan to carry out a more detailed study in the future.

#### 4. Conclusion

The correlation between the interfacial lithium-ion transfer resistance ( $R_{ct}$ ) and the double-layer capacitance ( $C_{dl}$ ) of the graphite composite electrodes coated with various SEIs was investigated. Different values of  $1/R_{ct}C_{dl}$  were found for each SEI and the frequency (or rate) of intercalation and de-intercalation of lithium-ions into graphite was found to be different. The activation energy of the interfacial ion transfer resistance was almost the same for all the electrolyte solutions. These results indicate that the pre-exponential factors of the Arrhenius equation of interfacial lithium-ion transfer in practical graphite anodes depend on the properties of SEI.

#### References

1. T. Fukutsuka, K. Koyamada, S. Maruyama, K. Miyazaki, and T. Abe, *Electrochim. Acta*, **199**, 380 (2016).
2. E. Peled, *J. Electrochem. Soc.*, **126**, 2047 (1979).
3. J. O. Besenhard, M. Winter, J. Yang, and W. Biberacher, *J. Power Sources*, **54**, 228 (1995).
4. G. Nazri and R. H. Muller, *J. Electrochem. Soc.*, **132**, 2050 (1985).
5. G. Nazri and R. H. Muller, *J. Electrochem. Soc.*, **132**, 1385 (1985).
6. K. Edström, M. Herstedt, and D. P. Abraham, *J. Power Sources*, **153**, 380 (2006).
7. D. Bar-Tow, E. Peled, and L. Burstein, *J. Electrochem. Soc.*, **146**, 824 (1999).
8. D. Aurbach, B. Markovsky, A. Shechter, and Y. Ein-Eli, *J. Electrochem. Soc.*, **143**, 3809 (1996).
9. K. Kanamura, H. Tamura, S. Shiraishi, and Z. Takehara, *J. Electrochem. Soc.*, **142**, 240 (1995).
10. D. Aurbach, K. Gamolsky, B. Markovsky, Y. Gofer, M. Schmidt, and U. Heider, *Electrochim. Acta*, **47**, 1423 (2002).
11. T. Sasaki, T. Abe, Y. Iriyama, M. Inaba, and Z. Ogumi, *J. Electrochem. Soc.*, **152**, A2046 (2005).
12. R. McMillan, H. Slegel, Z. X. Shu, and W. Wang, *J. Power Sources*, **81–82**, 20 (1999).
13. R. Mogi, M. Inaba, S.-K. Jeong, Y. Iriyama, T. Abe, and Z. Ogumi, *J. Electrochem. Soc.*, **149**, A1578 (2002).
14. A. Inoo, T. Fukutsuka, Y. Miyahara, K. Miyazaki, and T. Abe, *Electrochemistry*, **88**, 69 (2020).
15. Y. Wang, Y. Song, and Y. Xia, *Chem. Soc. Rev.*, **45**, 5925 (2016).
16. N. B. Luque and W. Schmickler, *Electrochim. Acta*, **71**, 82 (2012).
17. J. Seebeck, P. Schiffels, S. Schweizer, J.-R. Hill, and R. H. Meißner, *J. Phys. Chem. C*, **124**, 5515 (2020).
18. H. B. Son, M.-Y. Jeong, J.-G. Han, K. Kim, K. H. Kim, K.-M. Jeong, and N.-S. Choi, *J. Power Sources*, **400**, 147 (2018).
19. Y. Yamada, Y. Iriyama, T. Abe, and Z. Ogumi, *Langmuir*, **25**, 12766 (2009).
20. T. Abe, H. Fukuda, Y. Iriyama, and Z. Ogumi, *J. Electrochem. Soc.*, **151**, A1120 (2004).
21. Y. Yamada, F. Sagane, Y. Iriyama, T. Abe, and Z. Ogumi, *J. Phys. Chem. C*, **113**, 14528 (2009).
22. Y. Domi, M. Ochida, S. Tsubouchi, H. Nakagawa, T. Yamanaka, T. Doi, T. Abe, and Z. Ogumi, *J. Phys. Chem. C*, **115**, 25484 (2011).
23. Y. Domi, M. Ochida, S. Tsubouchi, H. Nakagawa, T. Yamanaka, T. Doi, T. Abe, and Z. Ogumi, *J. Electrochem. Soc.*, **159**, A1292 (2012).
24. S. Tsubouchi, Y. Domi, T. Doi, M. Ochida, H. Nakagawa, T. Yamanaka, T. Abe, and Z. Ogumi, *J. Electrochem. Soc.*, **160**, A575 (2013).
25. A. Profatlova, S.-S. Kim, and N.-S. Choi, *Electrochim. Acta*, **54**, 4445 (2009).